Prediction and measurement of blast induced rock fragmentation – A case study of Kajiado County quarries, Kenya

by E.K. Mutinda[1], B.O. Alunda[1], I.O. Ondicho[2], E. Agyekum[3]

Affiliation:
[1]School of Mines and Engineering, Taita Taveta University, Kenya
[2]School of Engineering, Dedan Kimathi University of Technology, Kenya
[3]University of Mines and Technology, Ghana

Correspondence to:
B.O. Alunda

Email:
benard.ouma@ttu.ac.ke

Dates:
Received: 11 May 2023
Revised: 21 Nov. 2024
Accepted: 21 Nov. 2024
Published: February 2025

How to cite:
Mutinda, E.K., Alunda, B.O., Ondicho, I.O., Agyekum, E. 2025. Prediction and measurement of blast induced rock fragmentation – A case study of Kajiado County quarries, Kenya. *Journal of the Southern African Institute of Mining and Metallurgy*, vol. 125, no. 2, pp. 113–120

DOI ID:
https://doi.org/10.17159/2411-9717/2803/2025

ORCiD:
E.K. Mutinda
https://orcid.org/0000-0002-1012-9655
B.O. Alunda
https://orcid.org/0000-0003-0283-6525
I.O. Ondicho
https://orcid.org/0000-0002-4488-5459
E. Agyekum
https://orcid.org/0009-0008-8485-3049

Abstract

Driven by the necessity to improve blast performance regarding fragment size distribution in limestone mines, this paper introduces the prediction and measurement of blast fragmentation distribution through the modified Kuz-Ram (MKR) and Kuznetsov-Cunningham-Ouchterlony (KCO) models. Precise prediction and measurement of rock fragmentation resulting from blasting play a critical role in hard rock ore extraction. This is due to the substantial influence of post-blast ore size distribution on the efficiency of all subsequent downstream rock handling and processing operations. Additionally, employing secondary breakage of boulders, when necessary, leads to an unjustified rise in production costs. In this paper, the MKR and KCO models were utilised to identify the most appropriate model for application in Bisil and Simba quarries situated in Kajiado County, Kenya. Split-Desktop was used for blast fragment measurement by processing digital images obtained after blasting and computing the fragment size distribution of the blasted rock. As per the investigation, the recorded percentages of boulders generated at the sites ranged from 7% to 12.3% for the Simba quarry and from 11.2% to 23.9% for the Bisil quarry, respectively. Regression, correlation, and root mean square error (RMSE) were employed as the primary performance indicators. The study concluded that KCO outperformed MKR in accurately predicting blast fragment sizes in the examined quarries.

Keywords

blasting, rock fragmentation, fragmentation model, split-desktop, particle size distribution

Introduction

Drilling and blasting in limestone mining act to minimise the size of rock to enable easy handling of the fragments in the downstream mining processes (Babaeian et al., 2019). Fragments of specific sizes are crucial in mining activities as they affect subsequent operations such as loading, hauling, and crushing. Precise measurement of rock fragmentation resulting from blasting, which is the initial stage of size reduction, is particularly significant in hard rock drilling and blasting (Gheibie et al., 2009). The distribution of rock sizes after blasting significantly impacts the effectiveness of all subsequent rock processing and comminution processes downstream (Abuhasel, 2019). In case there are too many fines or boulders, there is a direct economic liability to the mining company (Kanchibotla, Valery, and Morrell, 1999; Jahed Armaghani, 2018).

Several methods have been proposed for measuring blasted rock size distribution (Yusuf and Hashim, 2020). The sieve method provides a direct and precise method of measuring fragment sizes (Ouchterlony and Sanchidrián, 2019). However, the process is costly, time-consuming, and generally unrealistic for large-scale applications (Ouchterlony, 2005). Direct observation of the muck piles after blasting has also been used in the past but can only result in an approximation at best. The limitations of the sieve and observation methods can be overcome by the use of empirical models that have been developed by different researchers (Ouchterlony and Sanchidrián, 2019), as discussed in the theory section.

Kansake and other researchers in 2016, while studying fragmentation models in gold mines in Ghana, found that the distribution of the fines in a blast greatly influences the fragmentation models to be used (Kansake, Temeng, and Afum, 2016). Both Kuz-Ram and modified Kuz-Ram (MKR) provided a more accurate fragment size distribution prediction compared to Kuznetsov-Cunningham-Ouchterlony (KCO). The ability of these models to predict depends mainly on the geology of the rock and the blast design. Therefore, a more comprehensive study is needed to point out the most suitable empirical fragmentation model for sedimentary rocks. When planning hard rock mining using drilling and blasting methods, it is important to carry out fragmentation modelling for optimal material handling and informed control of blast output (Tosun and Konak, 2015).

An accurate model for predicting rock fragmentation is crucial for enhancing production efficiency during blasting operations. Factors such as geological conditions, geometric configurations, and explosive properties, including rock mass features, blast design, and explosive type, influence the distribution of blast fragment sizes (Hekmat, Munoz, and Gomez, 2019). Rock fragmentation influences the volumetric and packing properties of rocks (e.g., the fill factor and bulk volume) and therefore, the digging and hauling efficiency of the equipment utilised (Adebayo and Aladejare, 2013). Similarly, several studies have demonstrated the direct influence of the rock size distribution when fed into the crusher and mill processes on energy consumption, therefore, influencing the productivity of these processes (Latham and Lu, 1999; Tosun, 2018). Thus, blast fragmentation prediction and post-blast rock fragmentation measurements are identified as critical metrics in mining operation optimisation. With blasting affecting all the preceding downstream operations, including loading, hauling, and processing, there is a need for blasts to be designed and fragment sizes modelled to ensure that the selected blast parameters give the desired fragmentation.

Theory

Fragmentation models

The creation of fragmentation models arises from the necessity to offer engineering solutions to blasting challenges, including the optimisation of run-of-mine (ROM) fragmentation (Esen, 2013). Different models have been developed for fragment size distribution prediction from specific blast designs (Ouchterlony and Sanchidrián, 2019). Nevertheless, none of these models adeptly forecasts the size distribution resulting from a blast. The inputs for such models include explosive properties, the geometry of the blast design, and insitu rock properties.

Fragment size distribution prediction models are mainly classified into two broad groups, which consist of empirical and mechanistic models. Every model operates under its set of assumptions regarding the origins of fines production, whereas empirical models presume that finer fragmentation results from a heightened powder factor, characterised by increased input energy from explosives (Sanchidrián and Ouchterlony, 2017). On the contrary, mechanistic models attribute fines production to the physics and dynamics of detonation, as well as the transfer of blast energy during blasting. Consequently, their complexity and the requirement for intricate data render mechanistic models less favoured on mine sites (Cardu, Dompieri, and Seccatore, 2012).

Mechanistic models represent the pinnacle of modelling sophistication, showcasing progressive systems. They employ numerous numerical techniques and deliver blast predictions by accurately mimicking changes in conditions over time (Ouchterlony and Sanchidrián, 2019). By analysing stress or strain within the affected region, they have the capability to simulate the loading of bulk explosives and the movement of rocks around the blast area (Tosun and Konak, 2015). They are the most perplexing prediction models that are often used to describe the behaviour of complex system components, and some can take days or weeks to run even on powerful multi-centre or graphical user interface (GPU)-based computers (Raina, Murthy and Soni, 2015).

In contrast, empirical computer models rely on the direct fitting of scientific and computational expressions to data obtained from field measurements or potential estimation. Examples of these models incorporate the fracture forecast models and the scaled separation equation for predicting vibration (Abuhasel, 2019). Among these models is Da Gama's 1970 model, which forecasts fragment size distribution by considering the required energy and explosives, as well as rock characteristics (Ouchterlony and Sanchidrián, 2019). This model had the disadvantage of neglecting the effects of stemming length, spacing, and bench height and did not have factors for predicting the uniformity of the fragmented rocks. In 1973, Larsson developed another model, which utilised burden, spacing, specific charge and characteristics of the rock's discontinuities for prediction (Ouchterlony and Sanchidrián, 2019; Shehu, Yusuf and Hashim, 2020). This model was the earliest model to account for the uniformity index of blasted rock (Ouchterlony and Sanchidrián, 2019). In 1973, Kuznetsov introduced an empirical model that accounted for variables such as the type of explosives, rock mass classification, the impact of applied blast energy, and assessment of fragmentation uniformity. This model quantifies fragmentation in terms of mass percentage, powder factor (blast energy applied per unit volume of rock), and mean fragment size (Franklin and Maerz, 2018).

In 1983, Cunningham introduced the Kuz-Ram model, which could compute both the average fragment size and the uniformity index for the muck pile resulting from a bench blasting round. This model utilises the Rosin Rammler (RR) sieving curve function, which characterises fragmentation curves for equal mean size (Ouchterlony, 2019). In 1987, Kou and Rustan, working under the Swedish Detonic Research Foundation (SveDeFo) adjusted Larson's model (Ouchterlony, 2019). The main parameters considered were the bench height, stemming length, discontinuity characteristics, and the rock's nature. One of the drawbacks of the model was the approximation of the rocks' parameters leading to a lower value of the predicted dimensions of the rocks fragmented. (Gheibie et al., 2009).

In 2000, Chung and Katsabanis used Otterness' and other researchers' data collected in 1991 to verify the accuracy of the Kuz-Ram model (Ouchterlony, 2019). They proposed that the RR function gives a better representation of the fragment size distribution data (Ouchterlony and Sanchidrián, 2019). More advanced empirical models were developed with Kuznetsov-Cunningham-Ouchterlony (KCO) in 2005 and modified Kuz-Ram in 2009 (Ouchterlony and Sanchidrián, 2019). These models can often be represented in a spreadsheet and run on a laptop in almost no time (Monjezi et al., 2010).

Modified Kuz-Ram model

This empirical model closely resembles the previous Kuz-Ram model, with the only alteration being the adjustment of the Kuznetsov equation through the application of a 0.073 multiplier. This modification aims to enhance the model's accuracy in predicting the mean fragmentation size (Gheibie et al., 2009).

The Kuz-Ram uniformity index is further refined with an enhanced version proposed by Cunningham, which takes into account the blastability index (BI) of the specific rock under consideration (Ouchterlony and Sanchidrián, 2019). The model is made up of two main functions, namely the average broken rock size (X_m), as shown in Equation 1 and the modified uniformity index (n'). The input parameters of the two functions (X_m and n') are easy to obtain on-site, however, the model does not factor in the impact of blast timing, and the top size is also not well defined (Gheibie et al., 2009):

$$X_m = 0.073 \times BI \times \left(\frac{V_0}{Q_e}\right)^{0.8} \times (Q_e)^{\frac{1}{6}} \times \left(\frac{S_{ANFO}}{115}\right)^{-\frac{19}{30}} \qquad [1]$$

where X_m is the average broken rock size in cm, Q_e is the explosive weight per drill hole in kg. The broken rock volume per blast hole, V_0 (m^3) is, S_{ANFO} is the relative weight strength of the explosive to ANFO, and BI is the blastability index as shown in Equation 2:

$$BI = 0.5(HF + JPS + JPA + RDI + RMD) \quad [2]$$

where HF is the hardness factor, JPS is the joint plane spacing, JPA is the joint plane angle, RDI is the rock density influence, and RMD is the rock mass description (Bieniawski, 1988). These parameters are computed based on the rock mass classification introduced by Bieniawski in 1988, as outlined in Table 1.

The broken rock volume per blast hole V_0 (m^3) can be found by using Equation 3:

$$V_0 = B \times S \times H \quad [3]$$

where *B* is the blasting burden in m, S is the blast hole spacing in m, and H is the bench height in m. The uniformity index n is defined by Equation 4:

$$n = \left(2.2 - 14\frac{B}{D}\right)\sqrt{\frac{1+\frac{S}{B}}{2}}\left(1-\frac{W}{B}\right)\left(\frac{|BCL - CCL|}{|L|} + 0.1\right)^{0.1}\left(\frac{L}{H}\right) \quad [4]$$

where B is the blasting burden in m, D is the blast hole diameter in mm, S is the blast hole spacing in m, W is the drilling accuracy in m, BCL is the bottom charge length in m, and CCL is the column charge length in m, and H is the bench height in m, and L is the total charge length in m. When employing a staggered pattern, Equation 4 needs to be be multiplied by 1.1 (Gheibie et al., 2009).

The modified uniformity index (n') is shown in Equation 5.

$$n' = 1.88\,(BI)^{-0.12}\,n \quad [5]$$

KCO model

The Kuznetsov-Cunningham-Ouchterlony (KCO) fragmentation model extends the Kuz-Ram model by substituting the Rosin-Rammler equation with the Swebrec function (Ouchterlony and Sanchidrián, 2019). It was proposed to address two significant weaknesses of the Kuz-Ram model: its limited ability to accurately predict fragments with high fines, and its upper limit cut-off of block sizes (Ouchterlony, 2005). The Swebrec function shown in Equation 6 includes three parameters, the 50% passing (X_{50}), the maximum block size (X_{Max}), and b, which is a curve undulation parameter that depends on the uniformity index of the Kuz-Ram model (Franklin, 1993; Babaeian et al., 2019; Ouchterlony and Sanchidrián, 2019).

$$P_{(X)} = \frac{1}{\left\{1 + \left[\frac{\ln\left(\frac{X_{Max}}{X}\right)}{\ln\left(\frac{X_{Max}}{X_{50}}\right)}\right]^{b}\right\}} \quad [6]$$

where $P_{(x)}$ is the percentage fraction of fragments passing sieve size X, and b denotes the curve undulation parameter. X_{Max} stands for the minimum (insitu block size; S or B). The equations comprising the KCO models are illustrated in Equations 7 to 11.

$$X_{50} = A\left(\frac{1}{q^{0.8}}\right)Q^{\frac{1}{6}}\left(\frac{115}{S_{ANFO}}\right)^{\frac{19}{30}} \quad [7]$$

where A is the rock factor as shown in Equation 8, q is the specific charge/powder factor, kg/m^3, Q is the explosive weight per drill hole in kg, and S_{ANFO} is the relative weight strength of the explosive to ANFO.

Table 1

Rock mass classification

Parameter	Description	Rating
Rock mass description (RMD)	Powdery/friable	10
	Vertical joints	JF = JPS + JPA+ JCF
	Massive	50
Joint plane spacing (JPS)	Close (S_j < 0.1 m) S_j is the joint spacing	10
	Intermediate (0.1 < S_j < 0.3 m)	20
	Wide (0.3<S_j < 0.95 $\sqrt{BS}$)	50
	S_j >$\sqrt{BS}$. (where *BS* is reduced pattern)	80
Joint condition factor (JCF)	tight joints	1
	for relaxed joint	1.5
	gouge-filled joints	2
Joint plane angle (JPA) or joint plane orientation (JPO)	Horizontal	10
	Joints dip out of the face	20
	The strike is perpendicular/ normal to the face	30
	Joints dip into the face	40
Rock density influence (RDI) or specific gravity influence (SGI)		0.025ρ – 50 or 25SG – 50 (ρ is the density of the rock in kg/m^3 and SG is the specific density of rock in tonnes/cubic meters)
Hardness factor (HF)	Young's Modulus, E < 50 GPa	$\frac{E}{3}$
	Young's Modulus, E > 50 GPa	$\frac{\sigma_c}{5}$ (σ_c is the uniaxial compressive strength (UCS) in MPa)

$$A = 0.06(RMD + RDI + HF) \quad [8]$$

$$b = \left[2\ln 2\left(\ln\left(\frac{X_{Max}}{X_{50}}\right)\right)\right]n \quad [9]$$

Alternatively, the value of b can be determined by using Equation 10, as reported by Choudhary and Gupta (2012):

$$b = 0.5(D_{b50})^{0.25}\ln\left(\frac{D_{bMax}}{D_{b50}}\right) \quad [10]$$

where D_{bMax} is the least burden, spacing, or maximum insitu block size as suggested by Ouchterlony (2005) (Ouchterlony and Sanchidrián, 2019). The KCO model also gives an alternative equation for the X_{50} than originally proposed by the Kuz-Ram model as given in Equation 11.

$$X_{50} = \left(\frac{(\ln 2)^{\frac{1}{n}}}{\left(1+\frac{1}{n}\right)}\right) \times A \times \left(\frac{1}{q^{0.8}}\right) \times Q^{\frac{1}{6}} \times \left(\frac{115}{S_{ANFO}}\right)^{\frac{19}{30}} \quad [11]$$

However, Equation 11 reduces the fragment size distribution to smaller values, which leads to an increased percentage of fines. This drawback of Equation 11 led to the use of Equation 7 in this article for fragment size distribution.

Materials and method

This study was conducted at limestone quarries situated in Kajiado, as depicted in Figure 1. The management of these quarries falls under the purview of two companies: East African Portland Cement Company Ltd (EAPCC), which oversees operations in the Bisil quarries, while National Cement Company Limited (NCCL) operates the Simba Kajiado mine. Bisil quarry comprises four mining faces, whereas the Simba quarry consists of two mining faces, with extraction conducted in benches. Following the collection of bench data, blasting operations were conducted, and fragment images were captured for subsequent analysis using Split-Desktop software. In the Kajiado region, limestone and quartzite formations are typically bordered by semi-calcareous gneisses. The primary crystalline limestone is followed by a series of pelitic gneisses with minor calcareous and semi-pelitic layers. The basement system in the Kajiado region might be arranged into the accompanying transformed calcareous sediments, which comprise crystalline limestones and calc-silicate gneisses (see Figure 2). Even in areas surrounded by intensely migmatised gneisses, there has been minimal introduction of pegmatitic material into the limestones. The research methodology comprised the following steps:

- ➤ Fragmentation prediction involved the utilisation of both the modified Kuz-Ram model and the KCO model. Geotechnical data collection encompassed parameters, such as joint plane angle, hardness factor, rock density, joint plane spacing, and rock mass description for rock mass classification. Following that, the prediction of fragment sizes was conducted by applying Python code to implement the modified Kuz-Ram and KCO models. Quarry activities for data collection included identifying pushbacks, bench faces (as depicted in Figure 3), geological measurements, and capturing spatial and explosive parameters for each blast. Geological measurements were conducted to ascertain pre-existing fractures and their orientations. Additionally, joints on each bench face were identified, and distances between them were measured to determine the rock mass rating (RMR).
- ➤ Fragmentation analysis was conducted using image based particle tracking (IPT). Blast fragment images were captured using a digital camera and subsequently processed utilising Split-Desktop 4.0 software to ascertain fragment distribution.
- ➤ Comparative analyses of the prediction and measured results using statistical techniques. Regression, correlation, and root mean square error (RMSE) computations were applied to determine model performance indices. The performance indices helped identify the most suitable fragmentation model for the studied limestone mines.

Six blasts were examined for every quarry, and the process was repeated six times. The findings, which allow for the identification of blast performance at each quarry site in relation to the chosen empirical models, are provided in the results section.

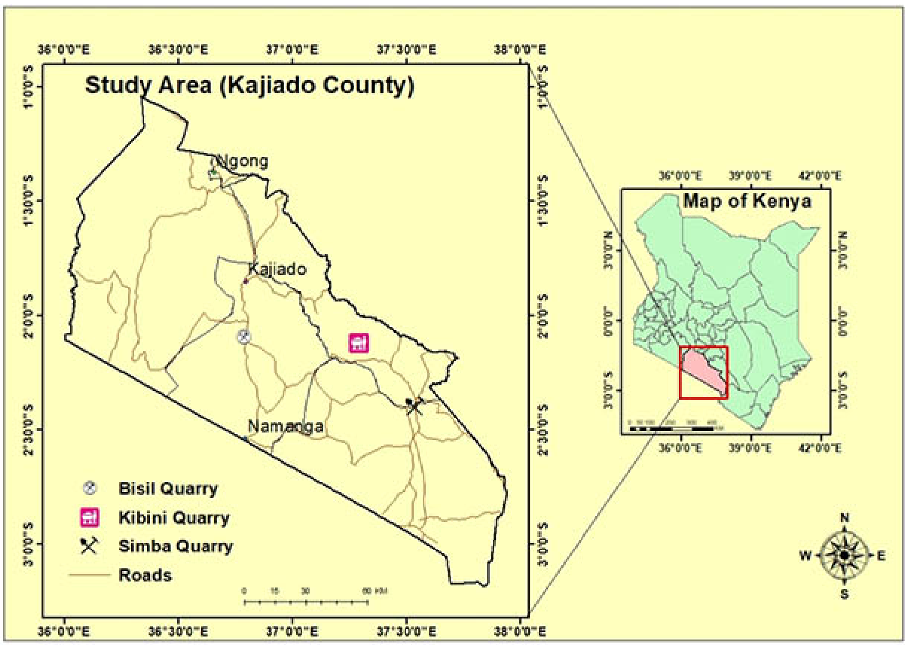

Figure 1—Study area

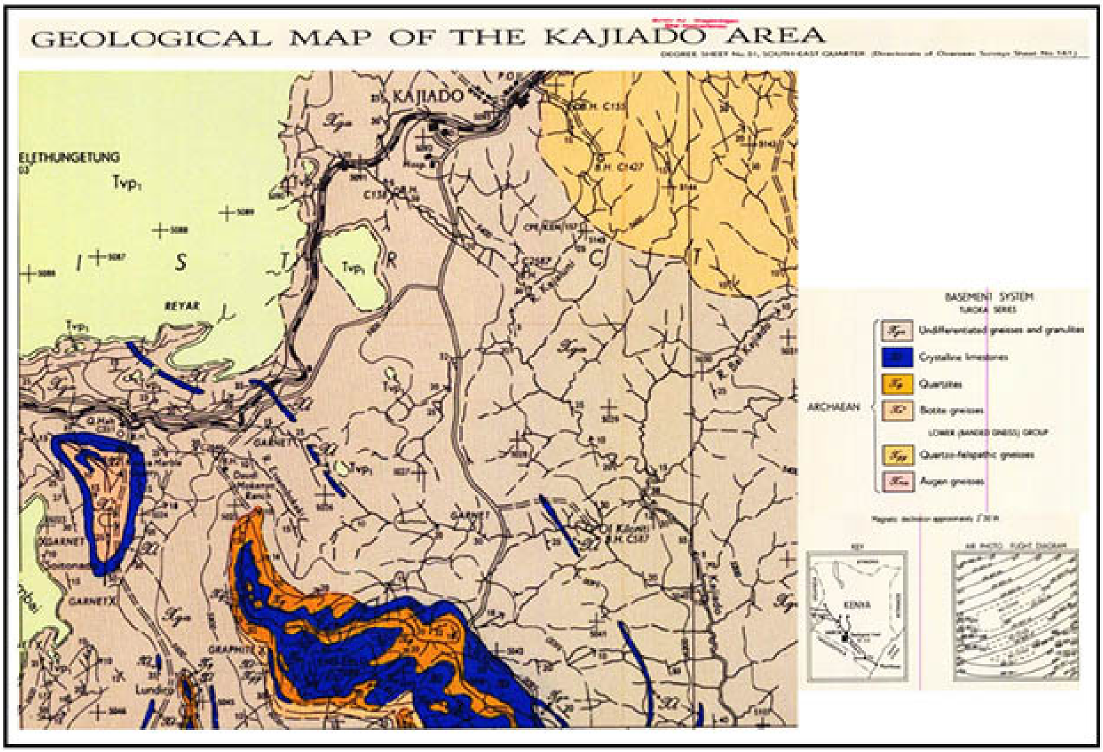

Figure 2—Geological map of Kajiado (Source: Geosociety organisation)

(a) (b)

Figure 3—The bench face of (a) Simba and (b) Bisil quarries before blasting showing joint orientation

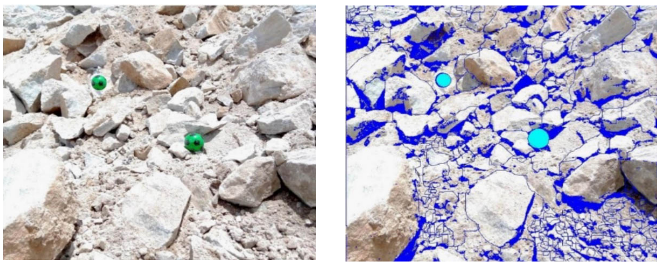

(a) (b)

Figure 4 —(a) The blasted rock taken from Simba quarry with scale objecy in place and (b) delineated image obtained using the Split Desktop 4.1

Results and discussion

Blast fragment size prediction by empirical modelling

The data for blast fragmentation prediction using empirical formulae were obtained from both the Simba and Bisil quarries, which were acquired through field measurements. The data included the geometrical, explosive and rock parameters as shown in Table 2 to Table 4. The rock mass was classified based on Bieniawski's geomechanical rock classification and the determination of the model's particle distribution was done using a code written in Python programming language.

Fragment size analysis by image processing

Even though the size distribution analysis by sieving is a direct and more accurate method, it is time-consuming and costly (Mohamed et al., 2015). It is also not practical for large-scale blasts. The only practical quantitative method of large-scale blast fragmentation analysis currently available is digital image processing, where photographs or video images are analysed via computer image processing software (Shehu, Yusuf, and Hashim, 2020). Digital image processing is used popularly in the mining industry because it is affordable, produces useful results, does not interrupt the production cycle, and is time efficient (Maerz, 1996). However, the method has a few setbacks compared to sieve analysis as it can only process the visible part of the muck pile (Shehu, Yusuf and Hashim, 2020). The sampling strategy is carefully considered, as image analysis processing techniques cannot take into account the internal muck pile structure (Sanchidrián, Segarra and López, 2006).

There exist several computer software for image analysis. These include SPLIT (e.g., Split Desktop), Wip Frag, Gold Size (Maerz, Palangio and Franklin, 1996), Frag Scan, TUCIPS, CIAS, Power Sieve, IPACS, KTH, and WIEP (Esen, 2013). In this research work the Split Desktop was used because of its availability, ease of use, and ability to produce reliable results (Júlio et al., 2019). The software employs grayscale to ascertain the particle size distribution of blast rock fragments (Júlio et al., 2019). Digital images were obtained using either a digital camera or smartphone. Multiple images were captured using a smartphone equipped with the Split Camera application, with a scale object included, as depicted in Figure 4 (a). High-quality images were transferred to a computer and those with a resolution of 600 dpi were delineated as shown in Figure 4 (b), to help determine blasted rock fragment size distribution using Split

Table 2
Rock Parameters used in the studied blast rounds

	Blast No.	Hardness factor	Joint plane spacing	Joint plane angle	Rock density influence	Rock mass rating	Specific gravity
Bisil	**1**	3.7	50.0	30.0	12.0	80.0	2.7
	2	4.1	20.0	30.0	13.0	80.0	2.7
	3	3.9	50.0	40.0	13.5	80.0	2.7
	4	4.0	50.0	30.0	12.5	80.0	2.7
	5	3.8	50.0	40.0	14.0	80.0	2.7
	6	4.0	50.0	30.0	12.0	80.0	2.7
Simba	**1**	3.5	20.0	40.0	13.5	60.0	2.5
	2	4.0	50.0	20.0	15.0	50.0	2.5
	3	4.3	50.0	30.0	13.8	50.0	2.4
	4	3.9	50.0	30.0	13.0	60.0	2.6
	5	4.0	20.0	20.0	13.6	50.0	2.5
	6	4.2	50.0	30.0	14.0	60.0	2.5

Table 3
Geometrical Parameters used in the studied blast rounds

	Blast No	Hole diameter (mm)	Spacing (m)	Bench height (m)	Burden (m)	Drilling deviation (m)	Hole depth (m)	Stemming (m)
Bisil	**1**	50.0	3.0	10.0	3.5	0.2	11.0	2.0
	2	50.0	3.0	10.0	3.5	0.2	11.0	2.0
	3	50.0	3.0	10.0	3.5	0.2	11.0	2.0
	4	50.0	3.0	10.0	3.5	0.1	11.0	2.0
	5	50.0	3.0	10.0	3.5	0.1	11.0	2.0
	6	50.0	3.0	10.0	3.5	0.2	11.0	2.0
Simba	**1**	50.0	3.5	6.0	2.5	0.1	6.0	1.5
	2	50.0	3.5	6.0	2.5	0.2	6.0	1.5
	3	50.0	3.5	6.0	2.5	0.1	6.0	1.5
	4	50.0	3.5	6.0	2.5	0.2	6.0	1.5
	5	50.0	3.5	6.0	2.5	0.1	6.0	1.5
	6	50.0	3.5	6.0	2.5	0.1	6.0	1.5

Table 4
Explosive parameters used in the studied blast rounds

Mine	Blast No	Powder factor (kg/m^3)	Explosive weight /hole (kg/hole)	Initiation system	Blasting pattern
Bisil	**1**	0.36	60.00	Nonel	Staggered
	2	0.35	65.00	Nonel	Staggered
	3	0.35	62.00	Nonel	Staggered
	4	0.35	64.00	Nonel	Staggered
	5	0.39	65.00	Nonel	Staggered
	6	0.37	60.00	Nonel	Staggered
Simba	**1**	0.37	45.00	electric	Staggered
	2	0.42	50.00	electric	Staggered
	3	0.40	47.00	electric	Staggered
	4	0.39	50.00	electric	Staggered
	5	0.39	49.00	electric	Staggered
	6	0.38	50.00	electric	Staggered

Desktop 4.1 software. After delineation was done, fragment size distribution was generated representing the measured fragment size distribution.

Statistical analysis of results

Correlation, regression, and root mean square error (RMSE) computations of the results obtained from the prediction models and the fragmentation measurements were conducted per quarry. They were presented in regression graphs measured against predicted results. Six blasts were considered for this research paper for both quarries. Simba quarry regression analysis showed KCO had a higher R^2 value than MKR in the blasts considered at 99.08% against 96.7%, respectively as illustrated in Figure 5 (a). The correlation analysis showed that there is a stronger correlation of KCO prediction to the measured fragment sizes than MKR prediction with a correlation value of 99.5% and 99.0%, respectively

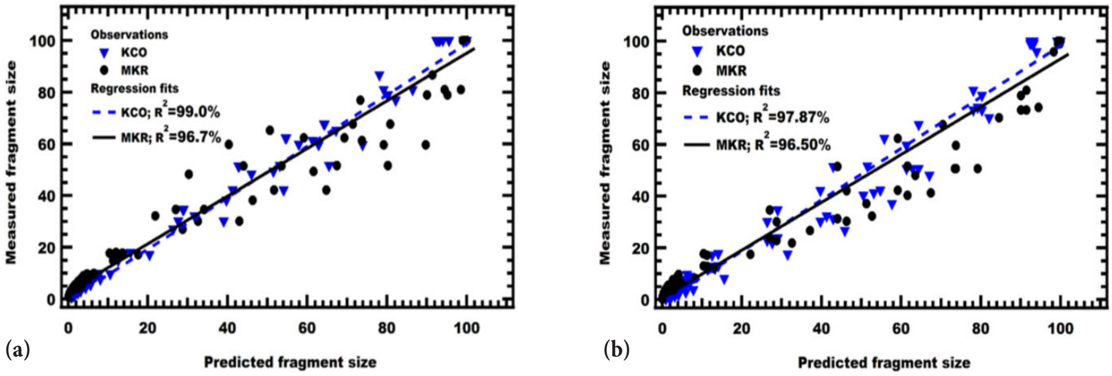

Figure 5—Regression graphs for (a) Bisil and (b) Simba quarries. KCO has a higher R^2 value at 97.87% and 99.08% compared to MKR at 96.50% and 96.74% for both quarries, respectively

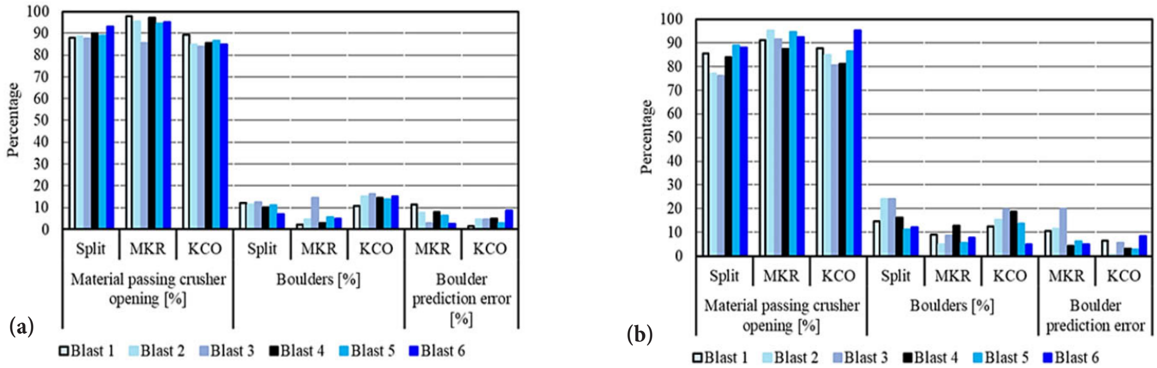

Figure 6—(a) Simba and (b) Bisil quarries material passing through crusher opening, boulder produced measurement and prediction analysis. It can be noted that the KCO graph almost resembles the Split Desktop graph, unlike the MKR graph. KCO also has the least error margin

for the same quarry. On the other hand, Bisil quarry regression analysis showed KCO had a higher R^2 value than MKR in five out of the six blasts considered. The overall regression analysis showed that KCO performed better than MKR with 97.9% against 96.5%, respectively as illustrated by Figure 5 (b). The correlation analysis showed that there is a stronger correlation between KCO prediction and MKR prediction with correlation values of 98.9% and 98.2%, respectively for the six blasts considered.

The RMSE results for Simba showed that KCO had the lowest RMSE at 3.8% compared to MKR whose RMSE was at 7.1% for the overall six blasts considered. On the other hand, the RMSE results for Bisil showed that KCO had the lowest error margin between 4.8% and 22.5% against MKR at 5.9% and 24.3% for the six blasts. The high correlation values indicate that all the predictions from the models correlated well with the actual results from the blasts studied. The maximum crusher feed for both quarries is 50 cm, where all materials of size greater than 50 cm were considered boulders. In Simba quarry, the KCO model showed better boulder prediction with an error margin between 1.6% to 8.7%, compared to MKR whose error margin was between 2.5% to 11.3% as illustrated by Figure 6 (a).

There was a general trend of overpredicting boulders by the KCO, while MKR underpredicted the number of boulders produced per blast round at Simba quarry, as can be seen in Figure 4 (a). KCO had a better boulder prediction in four blasts while MKR performed better in two out of the six blasts studied. A varying trend of boulder prediction was observed with MKR tending to underpredict the percentage of boulders, while KCO tended to overpredict the percentage of boulders produced per blast. According to Split Desktop, the percentage of boulders produced at the site was between 7.1% to 12.3%. This percentage is quite significant but not as much as the percentage of boulders produced at Bisil quarries. This could be attributed to the fact that Simba quarry has a better strategy for planning and executing blast rounds. However, the application of empirical fragment size modelling could reduce this percentage of boulders significantly. This can possibly be achieved by redesigning blast round parameters and simulating the new parameters using empirical models. Optimal parameters can thereafter be used in performing blasts for better fragmentation.

At Bisil quarry, the KCO model showed better boulder prediction with an error margin between 0.6% to 8.2% compared to MKR, of which the error margin was between 4.2% to 19.9% as illustrated by Figure 6 (b). However, there was a general trend of underpredicting boulders by the MKR while KCO overpredicted the percentage of boulders produced per blast round at Bisil quarry. According to Split Desktop, the percentage of boulders produced at the site was between 11.2% to 23.9%. The percentage of boulders is significant and thus has some negative impact on the overall mining cost as they will need to perform secondary blasting and also slow down the loading and hauling process. It was noted that KCO generally performed better in the prediction of boulders than MKR.

Conclusion

This research conducted a comparative analysis of two empirical blast fragmentation models in separate quarries in Kenya. The study highlights the superior predictive performance of the Kuznetsov-Cunningham-Ouchterlony (KCO) model over the modified Kuz-Ram (MKR) model in both boulder and overall particle size predictions. Interestingly, the prediction trends varied between the Bisil and Simba formations, indicating geological influence on model performance. Despite these variations, both MKR and KCO models offer valuable guidance on blast fragment particle size distribution, tailored to specific geological conditions and blast designs. This enables miners to assess different blast designs, explore the effects of altering blast variables, and predict resulting particle size distributions accurately. Mining operators can leverage empirical modelling as a tool to optimise blast round fragment size distribution. The observed tendency of boulder overestimation at Bisil quarry and underestimation at Simba quarry underscores the importance of accurate modelling. Notably, KCO exhibited stronger correlation, higher coefficient of determination, and lower error margins, reinforcing its reliability in predicting particle sizes. Moreover, variations in prediction trends across geological formations suggest that model performance is influenced by geological factors. Additionally, the relationship between powder factor and fragment sizes highlights the importance of considering blasting variables in fragmentation outcomes.

Acknowledgements

We express our sincere appreciation for the support provided by Split-Engineering for this project, particularly in granting the software license. Additionally, we extend our gratitude to the Exploration and Tertiary Material Department of East African Portland Cement Company (EAPCC) and the Mining Department of National Cement Company Ltd (NCCL) for their cooperation and for providing their personnel, equipment, and laboratory facilities for this research endeavour.

References

Abuhasel, K.A. 2019. A comparative study of regression model and the adaptive neuro-fuzzy conjecture systems for predicting energy consumption for jaw crusher. *Applied Sciences,* vol. 9, no. 18. doi: 10.3390/app9183916

Adebayo, B., Aladejare, A.E. 2013. Effect of Rock Properties on Excavation-Loading Operation in Selected Quarries. *Advanced Materials Research*, vol. 824, pp. 86–90. doi: 10.4028/www.scientific.net/AMR.824.86

Babaeian, M., Ataei, M., Sereshki, F., Sotoudeh, F., Mohammadi, S. 2019. A new framework for evaluation of rock fragmentation in open pit mines. *Journal of Rock Mechanics and Geotechnical Engineering*. Elsevier Ltd, vol. 11, no. 2, pp. 325–336. doi: 10.1016/j.jrmge.2018.11.006

Bieniawski, Z.T. 1988. The Rock Mass Rating (RMR) System (Geomechanics Classification) in Engineering Practice, in Kirkaldie, L. (ed.) *Rock Classification Systems for Engineering Purposes*. West Conshohocken, PA: ASTM International, pp. 17–34. doi: 10.1520/STP48461S

Cardu, M., Dompieri, M., Seccatore, J. 2012. Complexity analysis of blast-induced vibrations in underground mining: A case study. *International Journal of Mining Science and Technology*, vol. 22, no. 1, pp. 125–131.

Esen, S. 2013. Fragmentation modelling and the effects of ROM fragmentation on comminution circuits. *23rd International Mining Congress & exhibition of Turkey*, pp. 252–260.

Franklin, J.A. 1993. 32 - Empirical Design and Rock Mass Characterization, in FAIRHURST, C. (ed.) *Analysis and Design Methods*. Oxford: Pergamon, pp. 795–806. doi: https://doi.org/10.1016/B978-0-08-040615-2.50038-1

Franklin, J.A., Maerz, N.H. 2018. Empirical design and rock mass characterization. *Measurement of Blast Fragmentation*. Routledge, pp. 193–201. doi: 10.1201/9780203747919-28

Gheibie, S., Aghababaei, H., Hoseinie, S.H., Pourrahimian, Y. 2009. Modified Kuz-Ram fragmentation model and its use at the Sungun Copper Mine. *International Journal of Rock Mechanics and Mining Sciences*. Elsevier, vol. 46, no. 6, pp. 967–973. doi: 10.1016/j.ijrmms.2009.05.003

Hekmat, A., Munoz, S., Gomez, R. 2019. Prediction of Rock Fragmentation Based on a Modified Kuz-Ram Model. *Proceedings of the 27th International Symposium on Mine Planning and Equipment Selection - MPES 2018*. Cham: Springer International Publishing, pp. 69–79. doi: 10.1007/978-3-319-99220-4_6

Jahed Armaghani, D. 2018. Rock Fragmentation Prediction through a New Hybrid Model Based on Imperial Competitive Algorithm and Neural Network. *Smart Construction Research*, vol. 2, no. 3. doi: 10.18063/scr.v2i3.397

Júlio, S., Andrêvhity, S., Silva, S. 2019. Analysis of Blasting Rocks Prediction and Rock Fragmentation Results Using Split-Desktop Software. *Brazilian Association of Metallurgy, Materials and Mining*, vol. 15, no. 1, pp. 22–30.

Kanchibotla, S.S., Valery, W., Morrell, S. 1999. Modelling fines in blast fragmentation and its impact on crushing and grinding. *Explo 99–A conference on rock breaking, The Australasian Institute of Mining and Metallurgy*, Kalgoorlie, Australia, pp. 137–144.

Kansake, B.A., Temeng, V.A., Afum, B.O. 2016. Comparative Analysis of Rock Fragmentation Models – A Case Study. *4th UMaT Biennial International Mining and Mineral Conference*, no. September, pp. MP 1–11.

Latham, J.-P., Lu, P. 1999. Development of an assessment system for the blastability of rock masses. *International Journal of Rock Mechanics and Mining Sciences*, vol. 36, no. 1, pp. 41–55. doi: 10.1016/S0148-9062(98)00175-2

Maerz, N.H. 1996. Image sampling techniques and requirements for automated image analysis of rock fragmentation. *Proceedings of the FRAGBLAST 5 Workshop on Measurement of Blast Fragmentation*, Montreal, Quebec, Canada, pp. 115–120. doi: 10.1201/9780203747919-18

Maerz, N.H., Palangio, T.C., Franklin, J.A. 1996. WipFrag image based granulometry system. *Proceedings of the FRAGBLAST 5 Workshop on Measurement of Blast Fragmentation*, Montreal, Quebec, Canada, pp. 91–99. doi: 10.1201/9780203747919-15

Mohamed, F., Hafsaoui, A., Talhi, K., Menacer, K. 2015. Study of the Powder Factor in Surface Bench Blasting. *Procedia Earth and Planetary Science*, vol. 15, pp. 892–899. doi: 10.1016/j.proeps.2015.08.142

Monjezi, M., Amiri, H., Farrokhi, A., Goshtasbi, K. 2010. Prediction of Rock Fragmentation Due to Blasting in Sarcheshmeh Copper Mine Using Artificial Neural Networks. *Geotechnical and Geological Engineering*, vol. 28, no. 4, pp. 423–430. doi: 10.1007/s10706-010-9302-z

Ouchterlony, F. 2005. The Swebrec © function : linking fragmentation by blasting and crushing, 114 (March), pp. 29–44. doi: 10.1179/037178405X44539

Ouchterlony, F., Sanchidrián, J.A. 2019. A review of development of better prediction equations for blast fragmentation. *Journal of Rock Mechanics and Geotechnical Engineering*. Elsevier Ltd, vol. 11, no. 5, pp. 1094–1109. doi: 10.1016/j.jrmge.2019.03.001

Raina, A.K., Murthy, V.M. S.R., Soni, A.K. 2015. Flyrock in surface mine blasting: Understanding the basics to develop a predictive regime. *Current Science*, vol. 108, no. 4, pp. 660–665. doi: 10.18520/cs/v108/i4/660-665

Sanchidrián, J.A., Ouchterlony, F. 2017. A Distribution-Free Description of Fragmentation by Blasting Based on Dimensional Analysis. *Rock Mechanics and Rock Engineering*. Springer-Verlag Wien, vol. 50, no. 4, pp. 781–806. doi: 10.1007/s00603-016-1131-9

Sanchidrián, J.A., Segarra, P., López, L.M. 2006. A Practical Procedure for the Measurement of Fragmentation by Blasting by Image Analysis. *Rock Mechanics and Rock Engineering*, vol. 39, no. 4, pp. 359–382. doi: 10.1007/s00603-005-0073-4

Shehu, S.A., Yusuf, K.O., Hashim, M.H.M. 2020. Comparative study of WipFrag image analysis and Kuz-Ram empirical model in granite aggregate quarry and their application for blast fragmentation rating. *Geomechanics and Geoengineering*, pp. 1–9. doi: 10.1080/17486025.2020.1720830

Tosun, A. 2018. A modified Wipfrag program for determining muckpile fragmentation. *Journal of the Southern African Institute of Mining and Metallurgy*, vol. 118, no. 10, pp. 1113–1119. doi: 10.17159/2411-9717/2018/v118n10a13

Tosun, A., Konak, G. 2015. Determination of specific charge minimizing total unit cost of open pit quarry blasting operations. *Arabian Journal of Geosciences*, vol. 8, no. 8, pp. 6409–6423. doi: 10.1007/s12517-014-1657-7 ◆